Chinese Chemical Letters 36 (2025) 110067

Contents lists available at ScienceDirect

Chinese Chemical Letters

journal homepage: www.elsevier.com/locate/cclet

Injectable hydrogel-based tumor vaccine with fibrotic tumor immune microenvironment remodeling to prevent breast cancer postoperative recurrence and metastases

Honghao Sun, Huimin Zhao, Ronghui Yin, Chenxi Zhou, Ming Wu, Yueyang Deng, Zhanwei Zhou*, Minjie Sun*

NMPA Key Laboratory for Research and Evaluation of Pharmaceutical Preparations and Excipients, State Key Laboratory of Natural Medicines, Department of Pharmaceutics, China Pharmaceutical University, Nanjing 210009, China

ARTICLE INFO

Article history:
Received 30 March 2024
Revised 27 May 2024
Accepted 28 May 2024
Available online 29 May 2024

Keywords:
Injectable hydrogel
Tumor vaccine
Fibrosis
Breast cancer metastasis
BRD4

ABSTRACT

Postoperative recurrence and metastasis are still the main challenges of cancer therapy. Tumor vaccines that induce potent and long-lasting immune activation have great potential for postoperative cancer therapy. However, the clinical effects of therapeutic tumor vaccines are unsatisfactory due to immune escape caused by the lack of immunogenicity after surgery and the local fibrosis barrier of the tumor which limits effector T cell infiltration. To overcome these challenges, we developed an injectable hydrogel-based tumor vaccine, RATG, which contains whole tumor cell lysates (TCL), Toll-like receptor (TLR) 7/8 agonist imiquimod (R837) and an antifibrotic drug ARV-825. TCL and R837 were loaded onto the hydrogel to achieve a powerful reservoir of antigens and adjuvants that induced potent and lasting immune activation. More importantly, ARV-825 could be slowly and sustainably released in the tumor resection cavity to downregulate α-smooth muscle actin (α-SMA) and collagen levels, disintegrate fibrosis barriers and promote T cell infiltration after immune activation to reduce immune escape. In addition, ARV-825 also directly acted on the remaining tumor cells to degrade bromodomain-containing protein 4 (BRD4) which is a critical epigenetic reader overexpressed in tumor cells, inhibiting tumor cell migration and invasion. Therefore, our injectable hydrogel created a powerful immune niche in postoperative tumor resection cavity, significantly enhancing the efficacy of tumor vaccines. Our strategy potently activates the immune system and disintegrates the fibrotic barrier of residual tumors with immune microenvironment remodeling *in situ*, showing anti-recurrence and anti-metastatic effects, and provides a new paradigm for postoperative treatment of tumors.

Surgical resection is the main choice for clinical treatment of early and nonmetastatic solid tumors [1,2]. However, residual small tumors or circulating tumor cells can lead to fatal tumor recurrence and metastasis months or years after surgery [3]. Although >60% of patients with breast cancer or other solid tumors are treated with surgery, up to one-third patients experience fatal recurrence and metastasis due to the difficulty in detecting residual microscopic tumors and the postoperative immunosuppression [1,4]. Postoperative adjuvant chemotherapy and radiotherapy are standard treatment methods for postoperative cancer management; however, the side effects of chemotherapy and radiotherapy severely affect the quality of life of patients [3]. Although efforts of cancer immunotherapy have been made on tumor suppression and prevention of metastasis, lack of immunogenicity due to low tumor load after surgery and the serious fibrotic barrier on tumor resection cavity caused by residual tumor induction and surgical trauma stimulation, which inhibits immune cell infiltration, has hindered treatment efficiency [5-8].

During immune activation, antigens are essential for triggering immunogenicity [9]. Tumor vaccines developed using whole tumor cells represent a promising approach for cancer immunotherapy. The preparation of whole tumor cell vaccines does not require the identification of tumor antigens, which helps accelerate the preparation of tumor vaccines and achieve treatment goals earlier. Obviously, early intervention is beneficial in preventing recurrence and metastasis. Meanwhile, whole tumor cell vaccines provide a rich variety of known or unknown tumor-associated antigens from patients to achieve personalized treatment while reducing immune escape caused by tumor heterogeneity [10].

* Corresponding authors.
E-mail addresses: zwzhou@cpu.edu.cn (Z. Zhou), msun@cpu.edu.cn (M. Sun).

https://doi.org/10.1016/j.cclet.2024.110067
1001-8417/

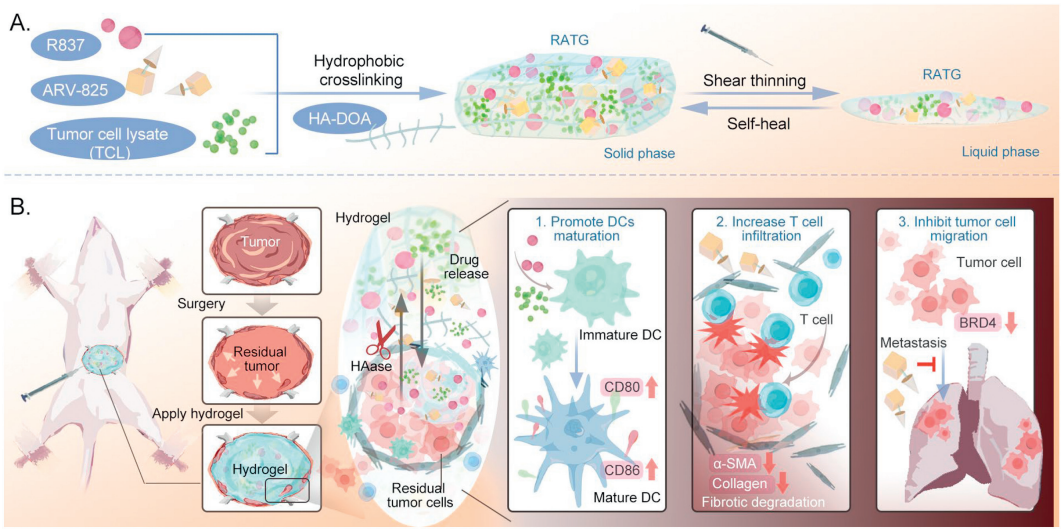

Scheme 1. Schematic illustration of the construction (A) and anti-tumor mechanism (B) of RATG.

After triggering immunogenicity, T cells proliferate and differentiate into effector T cells. Tumor infiltration effector T cells are the main immune cells that kill tumor cells. However, the fibrotic barrier in solid tumors can severely inhibit the infiltration of effector T cells and impair the effects of immunotherapy [11-14]. Therefore, disintegrating the fibrotic barrier and promoting immune cell infiltration are promising for enhancing the effect of immunotherapy. However, the removal of the fibrotic barrier can also free the tumor from binding and accelerate tumor metastasis [15,16]. Therefore, a combination of eliminating fibrosis and preventing metastasis may be a better choice. Fortunately, bromodomain-containing protein 4 (BRD4) may be a promising target. It is an important epigenetic reader, which is highly expressed in various tumors and fibrosis-related diseases [17-19]. It can promote the proliferation and migration of tumor cells, as well as the activation of fibroblasts. Notably, the proteolysis-targeting chimera (PROTAC) targeting BRD4, ARV-825, may be a good drug candidate, which can degrade BRD4 effectively and persistently [20].

An injectable hydrogel vaccine, RATG, containing whole tumor cell lysates (TCL), R837 and ARV-825, has been reported to overcome these challenges and prevent postoperative recurrence and metastasis of breast cancer. As illustrated in Scheme 1, TCL and the Toll-like receptor (TLR) 7/8 agonist R837 were loaded into the hydrogel as antigen and adjuvant, providing powerful antigen and adjuvant reservoirs, respectively, to induce lasting and powerful immune activation and avoid immune escape caused by low tumor antigen load after surgery and tumor heterogeneity. Meanwhile, ARV-825 can effectively degrade local tumor fibrosis and promote the infiltration of activated immune cells to play an effective immune-killing role. ARV-825 can also inhibit the migration and invasion of residual tumor cells and reduce the risk of metastasis after the removal of the fibrotic barrier. Local hydrogel administration can significantly improve the bioavailability of drugs in solid tumors, minimize systemic exposure, and reduce side effects in normal tissues. Our strategy enhances the effect of the tumor vaccine by simultaneously eliminating fibrosis and preventing metastasis, thus providing insights into the prevention of postoperative tumor recurrence and metastasis.

The synthesis of hydrogel matrix, dodecylamine (DOA) modified hyaluronic acid (HA) (HA-DOA), is illustrated in Fig. S1 (Supporting information). DOA, as a hydrophobic group, was coupled with HA through 4-(4,6-dimethoxy-1,3,5-triazin-2-yl)-4-methylmorpholinium chloride (DMTMM)-mediated amidation to obtain amphiphilic HA-DOA. The chemical structure and grafting rate of HA-DOA were verified using ^{1}H NMR spectroscopy. Peak *a* at 1.96 ppm corresponds to the acetyl group of HA, and peak *b* at 0.81 ppm corresponds to the terminal methyl group of DOA (Fig. 1A and Fig. S2 in Supporting information). By comparing the two integrated values, the grafting rate was calculated as approximately 20%. In addition, the successful synthesis of HA-DOA was also confirmed using Fourier transform infrared (FTIR) spectroscopy (Fig. S3 in Supporting information). Peaks at 2921.81 and 2852.76 cm^{-1} correspond to the symmetric and antisymmetric stretching vibration peaks of the methylene group in DOA, respectively. These two peaks also appeared in HA-DOA at 2923.97 and 2854.04 cm^{-1}.

According to our expectations, when the concentration of HA-DOA increased, hydrophobic interactions between the alkyl chains of DOA increased, which on the one hand, could form more cross-linking sites of the hydrogel through hydrophobic interactions, and on the other hand, could increase the interaction with hydrophobic drugs, enhancing drug loading and retention [21,22]. To demonstrate that, a fluorescence enhancement experiment with the fluorescent probe 8-aniline-1-naphthalenesulfonic acid (ANS) was carried out. When ANS is in water, its fluorescence is very weak, but in organic phase, it will be significantly enhanced [23]. As shown in Fig. S4 (Supporting information), with the concentration of HA-DOA increasing, the fluorescence intensity of ANS significantly increased at 450–550 nm, indicating that ANS was gradually entering into a hydrophobic environment; that is, hydrophobic interactions between HA-DOA increased gradually, which was beneficial for the formation of hydrogel cross-linking sites and loading of hydrophobic drugs [24,25].

Then the HA-DOA hydrogel and RATG were obtained by swelling lyophilized HA-DOA unloaded or loaded with drugs. As shown in Fig. 1B, when they were swollen at a concentration of 10 mg/mL, they appeared as solid hydrogels with limited fluidity. Next, scanning electron microscopy analysis demonstrated that the HA-DOA hydrogel and RATG possessed a porous network structure, which is a typical feature of hydrogels and makes them ideal drug reservoirs (Fig. 1C) [26].

In the case of surgery, the tumor resection cavity is an attractive site for local immunotherapy [27]. Traditional implantable hydrogels are useful in these cases [25]. However, injectable hydrogels continue to offer unique advantages in this area because they allow for easy administration, reduced invasiveness, and better coverage of irregular wounds owing to their deformability [28-30]. To

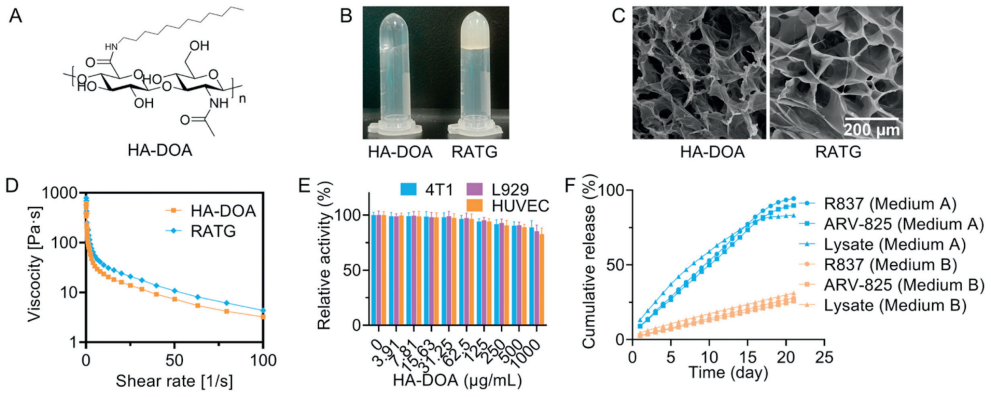

Fig. 1. Characterization of HA-DOA and RATG. (A) The structure of HA-DOA. (B) Images of HA-DOA hydrogel and RATG. (C) Scanning electron microscope (SEM) of HA-DOA hydrogel and RATG. Scale bar: 200 μm. (D) Viscosity of the HA-DOA hydrogel and RATG as a function of shear rate at 25 °C. (E) The biosafety of HA-DOA ($n = 6$). (F) The drugs release from RATG (medium A and medium B correspond to 800 ng/mL and 150 ng/mL HAase in pH 6.5 PBS, respectively). Data are shown as mean ± SD.

study the injectability of our hydrogel, the rheological properties of the HA-DOA hydrogel and RATG were investigated. First, their shear-thinning properties were evaluated. An increase in the shear rate led to a gradual decrease in the viscosity of both the hydrogels (Fig. 1D), indicating that when hydrogels are subjected to increased shear force during injection, their viscosity can be reduced to facilitate injection [31,32]. It was worth noting that the presence of the drugs had no significant effect on the shear-thinning properties of the hydrogels, which indicated the drug-loading adaptability of HA-DOA hydrogel. Next, the changes in the storage modulus and elastic modulus of the two hydrogels under different strains were examined. With increasing strain, the storage modulus of the hydrogels gradually changed from less than the elastic modulus to greater than the elastic modulus, indicating that the hydrogels changed from solid- to fluid-like (Fig. S5 in Supporting information). This phenomenon also supports their injectability. Because the hydrogel needs to return to the gel state after injection to maintain the slow and long-term release of drugs [33], we investigated the recovery ability of hydrogel. At a high strain, the storage modulus was higher than the elastic modulus, and the hydrogel appeared to be in a solution state. However, the elastic modulus and storage modulus quickly recovered after the high strain was removed, and the hydrogel appeared to be in a gel state (Fig. S6 in Supporting information). That is to say, the material can quickly return to a gel state after injection, thereby preventing drug leakage and ensuring the long-term slow release of drugs. Finally, in the real injectability tests (Fig. S7 in Supporting information), both hydrogels could be injected into saline through a 1-mL syringe needle (27 G) without blocking or collapsing (stained with crystal violet for visualization). In summary, the HA-DOA hydrogel and RATG have excellent injectability due to their shear-thinning properties and self-healing ability, allowing RATG to serve as an ideal injectable drug reservoir without drug leakage.

Next, the biosafety of HA-DOA in 4T1, L929, and human umbilical vein endothelial cells (HUVEC) cell lines was studied. Even at 1 mg/mL, all three cell types maintained a survival rate greater than 80%, indicating the good biosafety of the hydrogel matrix (Fig. 1E). Hemolysis assays were also performed to evaluate the biosafety of the HA-DOA. The hemolytic effect of HA-DOA on red blood cells was negligible (Fig. S8 in Supporting information). These results verified that the HA-DOA hydrogel has good biosafety in clinical and biomedical applications for cancer treatment.

The *in vitro* degradability of HA-DOA hydrogel was also studied. As shown in Fig. S9 (Supporting information), the molecular weight of HA-DOA decreased gradually after incubation with 800 ng/mL hyaluronidase (HAase) for 24 and 48 h, indicating that HA-DOA could be effectively degraded by HAase. Subsequently, we carried out *in vivo* degradation experiments, as shown in Fig. S10 (Supporting information), with the passage of time, the residual hydrogel gradually decreased, indicating its good biodegradability *in vivo*. All animal experiments were performed under the guidance and approved by the Ethics Committee of China Pharmaceutical University.

After HA-DOA was confirmed to be non-cytotoxic, the effect of drug-loaded RATG on tumor cells was evaluated. As a PROTAC targeting BRD4, ARV-825 can efficiently and durably degrade BRD4 and thus inhibit tumor cell growth. Therefore, the growth inhibitory capacity of RATG was first evaluated on murine breast cancer cells (4T1). Free ARV-825 and RATG showed similar growth inhibition abilities in 4T1 cells, indicating that RATG could inhibit tumor cell growth as effectively as ARV-825 (Fig. S11 in Supporting information).

Next, the *in vitro* drugs release from RATG was evaluated. In the tumor microenvironment, the high expression of HAase [34] may lead to the degradation of the hydrogel matrix HA-DOA, prompting the release of drugs from the hydrogel, and making RATG exhibit tumor microenvironment responsiveness. To evaluate the drug release properties of RATG, we performed *in vitro* release tests at different HAase concentrations. As shown in Fig. 1F, at high concentration of HAase that simulated the tumor microenvironment, the releases of drugs in RATG were significantly faster than that in the low concentration group which simulated the normal tissues, indicating the responsive capability of RATG to tumor microenvironment, which will help reduce toxicity to normal tissues. Importantly, although RATG released the drugs relatively rapidly at high concentrations of HAase, the release was still maintained for nearly three weeks, indicating the potential for lasting activation of the immune system.

The migration and invasion behaviors of tumor cells are closely related to metastasis in patients with cancer. Therefore, we evaluated the anti-migration and anti-invasion capabilities of RATG through *in vitro* scratch assay and Transwell invasion assay. The untreated scratch recovered significantly after 24 h, however, the free ARV-825 and RATG groups showed obvious lower relative migration ability of 22% and 23%, respectively (Fig. 2A and Fig. S12 in Supporting information). The results showed that RATG could weaken the migration ability of tumor cells, thereby reducing the occurrence of metastasis. The Transwell assay was used to evaluate the anti-invasive activity of RATG. In phosphate buffered saline (PBS) group, a large number of tumor cells passed through Matrigel from the upper chamber (Fig. 2B and Fig. S13 in Supporting information). However, free ARV-825 and RATG showed obvious invasion inhibition with only 27% and 25% relative invasion, respectively. The above results together indicate that RATG has good anti-

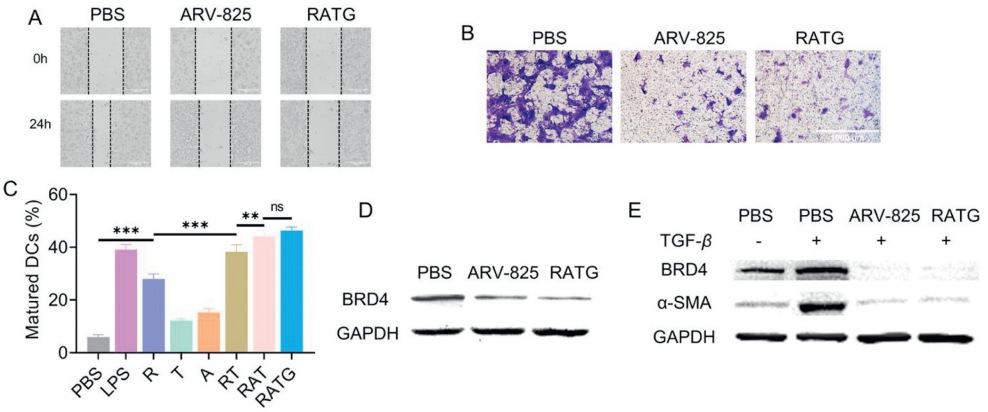

Fig. 2. *In vitro* biological effect evaluation. (A) Inhibition of migration *in vitro*. Scale bar: 500 μm. (B) Inhibition of invasion *in vitro*. Scale bar: 1000 μm. (C) DC maturation *in vitro*. (D) Degradation of BRD4 on 4T1. (E) Degradation of BRD4 and expression of α-SMA on NIH 3T3. Data are shown as mean ± SD. $^{**}P < 0.01$, $^{***}P < 0.001$. ns, no significant difference. GAPDH, glyceraldehyde 3-phosphate dehydrogenase.

migration and anti-invasion ability *in vitro* and has the potential for anti-metastasis after surgery.

In order to confirm the anti-migration and anti-invasion mechanism of RATG, we studied the effect of RATG on the expression of BRD4 *in vitro*. As an important epigenetic reader, BRD4 is highly expressed in breast cancer and regulates tumor proliferation, migration and invasion [35,36]. As a BRD4-targeting PROTAC, ARV-825 can effectively degrade BRD4 [20]. Therefore, we verified the BRD4 degrading effect of RATG on 4T1 tumor cells by Western blot. Untreated 4T1 cells showed high BRD4 expression, but treatment with free ARV-825 or RATG significantly reduced BRD4 expression (Fig. 2D). This showed that RATG can reduce BRD4 levels in 4T1 tumor cells as effectively as ARV-825 and thus inhibit tumor cell migration and invasion. In addition, BRD4 is also highly expressed on tumor-associated fibroblasts and upregulates the expression of α-smooth muscle actin (α-SMA) to promote tumor fibrosis [37]. Therefore, we also examined the effect of RATG on the expression of BRD4 and α-SMA on transforming growth factor-β (TGF-β)-induced NIH 3T3 fibroblasts by Western blot. As shown in Fig. 2E, TGF-β could significantly induce the upregulation of BRD4 and α-SMA on NIH 3T3 cells, while ARV-825 and RATG can effectively block this process. The above results collectively indicate that RATG has both anti-fibrosis and anti-metastasis capabilities, which helps to reduce the risk of metastasis in anti-fibrosis strategies for tumor treatment.

Dendritic cells (DCs) are the most powerful antigen-presenting cells. Activated DCs deliver ingested tumor-associated antigens to effector T cells, which initiate tumor-killing immunity. To test whether our vaccine enhanced DC activation, DC2.4 cells were treated with PBS, positive control lipopolysaccharide (LPS), adjuvant R837 (R), TCL (T), ARV-825 (A), R837 + TCL (RT), R837 + TCL + ARV-825 (RAT), and RATG for 24 h. The expression of CD80 and CD86 in DC2.4 cells was detected by flow cytometry. Without the adjuvant, TCL alone induced limited DC maturation (12.1%; Fig. 2C and Fig. S14 in Supporting information). Although only R837 can induce 27.1% of DCs to mature without antigen, DCs cannot perform the antigen presentation to T cells, and thus, cannot complete the subsequent immune killing to tumor cells. Therefore, the combination of antigens and adjuvants is necessary. In addition, their combined use further promoted DC maturation (37.0%). The presence of ARV-825 had no negative effect on R837- and TCL-induced DC maturation, indicating that RATG could effectively promote DC maturation *in vitro* and be a promising tumor vaccine. The secretion of IL-12 also confirmed that DCs was effectively activated by RATG (Fig. S15 in Supporting information).

Conventional vaccines may only provide antigens for a few days after a single dose, which is much shorter than the weeks of exposure to a natural infection [24,25]. This is one of the reasons why some tumor vaccines are less effective. To address this problem, vaccines loaded into hydrogels were developed. To achieve lasting therapeutic effects, drug-loaded gels, which serve as drug reservoirs, must sustainably release drugs. To verify this *in vivo*, we replaced the drugs with a hydrophobic fluorescent dye IR780, labeled TCL with Cy3.5, loaded them into the hydrogel, and administered it. Then, we evaluated drug retention in the hydrogel through an *in vivo* imaging system. As shown in Figs. 3A and B, free payloads underwent fast metabolism within several days, whereas payloads in the hydrogel maintained strong retention for >2 weeks, indicating the good retention ability of RATG.

To investigate the anti-recurrence and anti-metastatic ability of RATG *in vivo*, we constructed a 4T1 orthotopic breast cancer model. Because micrometastases usually occur when the tumor volume reaches approximately 500 mm^3 [3,38], we performed surgery to remove the primary tumor when tumor reached this size. The next day, the therapeutic agents were injected into the tumor resection cavity to evaluate their ability to inhibit recurrence and distant metastasis. As shown in Figs. 3C and D, the tumor relapsed rapidly in the saline group. In the ATG (RATG without R837) group, tumor recurrence was slightly suppressed, probably due to the direct antitumor effect of ARV-825 alone, while the immune system could not be activated efficiently due to the absence of adjuvant R837. In the RTG (RATG without ARV-825) group, although the immune system could be activated in the presence of antigen and adjuvant, the therapeutic effect was not satisfactory, probably because the fibrotic barrier of solid tumors inhibited the infiltration of immune cells. As the primary tumor was resected, the antigen load in the tumor resection cavity was relatively low. Thus, the RAG (RATG without TCL) group showed a moderate antitumor effect because the antigen presentation to effector T cells was insufficient. In the RAT (RATG without HA-DOA hydrogel) group, because the drugs and antigens could be cleared quickly, the immune system could not be effectively activated, the antitumor and antifibrotic effects of ARV-825 could not be maintained, thus the antitumor effect was also relatively weak. RATG group showed the best anti-relapse effect, on the one hand, due to its continuous antigen and adjuvant release, which can effectively activate the immune system, on the other hand, the anti-fibrosis effect of ARV-825 can promote the infiltration of effector T cells and enhance immune killing. In addition, the direct tumor-suppressive effect of ARV-825 could be also responsible for the therapeutic effect. The H&E staining of tumors also demonstrated the necrosis of the tumor cells after the RATG

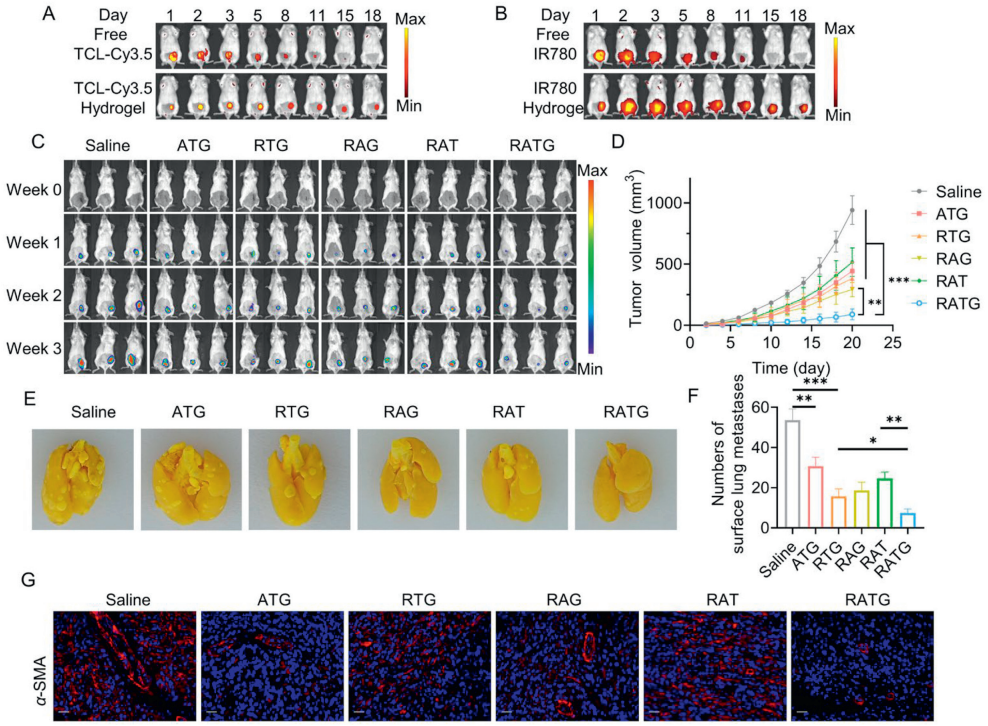

Fig. 3. (A) *In vivo* retention of TCL in hydrogel. (B) *In vivo* retention of drugs in hydrogel. (C) *In vivo* bioluminescence images to evaluate the recurrence of 4T1-Luc tumor after various treatments. (D) The tumor volume after various treatments ($n = 6$). (E) Photographs of *ex-vivo* lungs tissues after various treatments. (F) The number of surface lung metastasis ($n = 6$). (G) α-SMA immunofluorescence staining of tumors after various treatments. Scale bar: 20 μm. Data are shown as mean ± SD. $^{*}P < 0.05$, $^{**}P < 0.01$, $^{***}P < 0.001$.

treatment (Fig. S16 in Supporting information). There was no remarkable change in the body weight of mice treated with various preparations, indicating the good biosafety of them (Fig. S17 in Supporting information). We also evaluated the biosafety of RATG in healthy mice. Compared with saline treatment, there were no significantly different in H&E staining of major organs and blood biochemistry, further indicating the biosafety of RATG (Figs. S18 and S19 in Supporting information).

The lung tissues were harvested and stained to evaluate the anti-metastatic effects after mice were sacrificed. A large number of lung metastases were observed in the saline group (Figs. 3E and F). However, the group with long-term release of ARV-825 (ATG) or sustained release of antigens and adjuvants (RTG) showed varying degrees of reduction, respectively, indicating that the long-lasting release of ARV-825 had an anti-metastatic effect *in situ*, and the systemic immunity activated by the vaccine could also inhibit distant metastasis. The RATG group exhibited immunotherapeutic, antifibrotic, and *in situ* antimetastatic effects, and therefore had the best antimetastatic effect and reduced lung metastasis by 86%. The H&E staining of lungs also exhibited similar results (Fig. S20 in Supporting information).

In terms of survival time, consistent with the antirelapse and antimetastatic results, the median survival time was 28 days and 66 days in the saline and RATG groups, respectively, proving the superiority of RATG (Fig. S21 in Supporting information).

To evaluate the antifibrotic effect of the various preparations, Masson's trichrome staining and α-SMA staining were performed on dissected tumor tissue sections. In Masson's trichrome staining experiments, the collagen fibers were stained blue. In the group without sustained ARV-825 release (saline, RTG, and RAT), significantly more blue areas were observed, suggesting the severity of breast cancer fibrosis (Fig. S22 in Supporting information). In the group with sustained ARV-825 release (ATG, RAG, and RATG), significantly fewer blue areas were observed, indicating the impact of ARV-825 on fibrosis. Similar results were obtained in studies of α-SMA, demonstrating that sustained ARV-825 release can exert a potent antifibrotic effect on tumor tissue (Fig. 3G).

To better understand the antitumor effect of our vaccine, we analyzed the activation and infiltration of immune cells in the lymph nodes and tumor tissues. The proportion of mature DCs in lymph nodes was significantly upregulated in the RATG group (28.5%) compared with the saline group (14.5%), suggesting that RATG can more effectively promote DC maturation (Figs. 4A and B). Mature DCs prime effector T cells, increasing the proportion of $CD8^+$ T cells and thus killing residual and metastatic tumor cells. Therefore, we investigated the infiltration of $CD8^+$ T cells into the tumor. Due to the sustained-release antigens and adjuvants, the proportion of intratumoral $CD8^+$ T cells in the RTG group reached 17.3%, which was higher than 10.3% in the saline group, but significantly lower than 29.7% in the RATG group, due to the absence of the inhibitory effect of ARV-825 on fibrosis (Figs. 4C and D). We also evaluated the infiltration of $CD8^+$ T cells into the tumor using immunofluorescence staining (Fig. S23 in Supporting information). The results were similar to that of flow cytometry. We also evaluated the proportion of regulatory T cell (Treg) cells that play an immunosuppressive role in tumors. A large proportion of Treg cells were present in immunosuppressed fibrotic tumors (Figs. 4E and F). RATG treatment significantly decreased the Treg ratio from 43.2% to 8.31% compared with the saline group, which may be attributed to long-lasting immune activation and the elimination of fibrotic tumor matrix after RATG treatment. In addition, compared with the saline group, the levels of tumor necrosis factor-α (TNF-α), interferon-γ (IFN-γ) and granzyme B secreted by activated immunocytes increased 8.1-, 4.6- and 4.1-fold, respectively, in the RATG group, further confirming the potent immune activation effect of RATG (Fig. S24 in Supporting information).

In this work, a hydrogel-based tumor vaccine containing adjuvant, whole tumor cell lysates and antifibrotic drug was developed

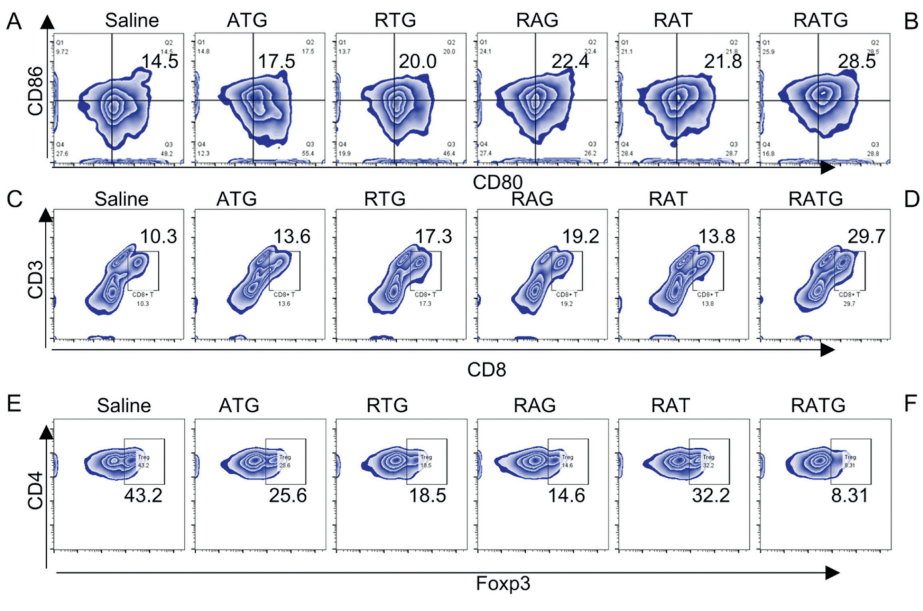

Fig. 4. Immune activation *in vivo*. (A) DC maturation in lymph nodes. (B) Statistical analysis of (A) ($n = 3$). (C) Proportion of infiltrating $CD8^+$ T cells in tumors. (D) Statistical analysis of (C) ($n = 3$). (E) Proportion of infiltrating Treg cells in tumors. (F) Statistical analysis of (E) ($n = 3$). Data are shown as mean ± SD. $^{**}P < 0.01$, $^{***}P < 0.001$.

to prevent the postoperative recurrence and metastasis of breast cancer. The hydrogel-based tumor vaccine can form a reservoir and sustain cargos release for up to 2 weeks with good biosafety. The reservoir can potently and persistently activate the immune system while locally producing an antifibrotic effect on the residual tumor tissue to promote the infiltration of activated immune cells and amplify the effects of immunotherapy. Moreover, the antifibrotic drug ARV-825 can also directly inhibit the growth, migration and invasion of residual tumor cells, and together with immunotherapy reduce tumor recurrence and metastasis after surgery.

In summary, combining antifibrotic strategies with whole tumor cell vaccines can effectively alleviate the postoperative recurrence and metastasis of breast cancer, providing new insights into the postoperative treatment of breast cancer.

Declaration of competing interest

The authors declare that they have no known competing financial interests or personal relationships that could have appeared to influence the work reported in this paper.

CRediT authorship contribution statement

Honghao Sun: Writing – original draft, Methodology, Investigation, Conceptualization. **Huimin Zhao:** Methodology, Investigation. **Ronghui Yin:** Methodology, Investigation. **Chenxi Zhou:** Methodology, Investigation. **Ming Wu:** Methodology. **Yueyang Deng:** Methodology. **Zhanwei Zhou:** Writing – review & editing, Methodology, Funding acquisition, Conceptualization. **Minjie Sun:** Writing – review & editing, Funding acquisition, Conceptualization.

Acknowledgments

This work was financially supported by the National Natural Science Foundation of China (No. 82102202), Key Research and Development Program Social Development Project of Jiangsu Province (No. BE2023845) and Natural Science Foundation of Jiangsu Province (No. BK20210424). We would like to thank Xiaonan Ma of China Pharmaceutical University for providing technical assistance of Carl Zeiss LSM 800 on the Public Experimental Platform. We also would like to thank Lin Ge of Animal Experimental Center in China Pharmaceutical University for kind help in the *in vivo* experiments.

Supplementary materials

Supplementary material associated with this article can be found, in the online version, at doi:10.1016/j.cclet.2024.110067.

References

[1] J.G. Hiller, N.J. Perry, G. Poulogiannis, B. Riedel, E.K. Sloan, Nat. Rev. Clin. Oncol. 15 (2018) 205–218.
[2] H. Liu, X. Shi, D. Wu, et al., ACS Appl. Mater. Interfaces 11 (2019) 19700–19711.
[3] T. Wang, D. Wang, H. Yu, et al., Nat. Commun. 9 (2018) 1532.
[4] F. Tang, Y. Tie, C. Tu, et al., Clin. Transl. Med. 10 (2020) 199–223.
[5] J. Dong, C. Zhu, Y. Huang, et al., Acta Pharm. Sin. B 13 (2023) 3106–3120.
[6] Z. Li, Y. Wang, Y. Shen, et al., Sci. Adv. 6 (2020) eaaz9240.
[7] T. Hata, K. Kawamoto, H. Eguchi, et al., Pancreas 46 (2017) 1259–1266.
[8] Z. Lu, J. Zou, S. Li, et al., Nature 579 (2020) 284–290.
[9] X. Chen, Z. Jiang, Y. Lin, et al., J. Control. Release 358 (2023) 345–357.
[10] J.L. Tanyi, S. Bobisse, E. Ophir, et al., Sci. Transl. Med. 10 (2018) eaao5931.
[11] B. Piersma, M.K. Hayward, V.M. Weaver, Biochim. Biophys. Acta Rev. Cancer 1873 (2020) 188356.
[12] H.F. Dvorak, Cancer Immunol. Res. 3 (2015) 1–11.
[13] B. Rybinski, J. Franco-Barraza, E. Cukierman, Physiol. Genomics 46 (2014) 223–244.
[14] H. Hu, W. Zhang, L. Lei, et al., Chin. Chem. Lett. 35 (2024) 108765.
[15] H. Jiang, S. Hegde, D.G. DeNardo, Cancer Immunol. Immun. 66 (2017) 1037–1048.
[16] I. Leake, Nat. Rev. Gastroenterol. Hepatol. 11 (2014) 396.
[17] A. Saraswat, M. Patki, Y. Fu, et al., Nanomedicine 15 (2020) 1761–1777.
[18] S. Sato, K. Koyama, H. Ogawa, et al., Respir. Investig. 61 (2023) 781–792.
[19] S. Sdelci, A.F. Rendeiro, P. Rathert, et al., Nat. Genet. 51 (2019) 990.
[20] J. Lu, Y. Qian, M. Altieri, et al., Cell Chem. Biol. 22 (2015) 755–763.
[21] S. Trombino, C. Servidio, F. Curcio, R. Cassano, Pharmaceutics 11 (2019) 407.
[22] D.L. Taylor, M.I.H. Panhuis, Adv. Mater. 28 (2016) 9060–9093.
[23] N. Liu, L. Zhu, H. Sun, et al., Adv. Healthcare Mater. 11 (2022) 2102329.
[24] G.A. Roth, E.C. Gale, M. Alcantara-Hernandez, et al., ACS Cent. Sci. 6 (2020) 1800–1812.
[25] S. Correa, A.K. Grosskopf, H.L. Hernandez, et al., Chem. Rev. 121 (2021) 11385–11457.
[26] Q. Li, Q. Song, Z. Zhao, et al., ACS Nano 17 (2023) 10376–10392.
[27] J. Wang, Y. Zhang, J. Pi, D. Xing, C. Wang, J. Control. Release 340 (2021) 149–167.
[28] C. Liu, Y. Liao, L. Liu, et al., Front. Bioeng. Biotechnol. 11 (2023) 1121887.
[29] R. Tian, X. Qiu, W. Mu, et al., Chin. Chem. Lett. 35 (2024) 108343.

[30] H. Song, P. Huang, J. Niu, et al., Biomaterials 159 (2018) 119–129.
[31] J. Pupkaite, J. Rosenquist, J. Hilborn, A. Samanta, Biomacromolecules 20 (2019) 3475–3484.
[32] F. Shuai, Y. Zhang, Y. Yin, H. Zhao, X. Han, Carbohydr. Polym. 260 (2021) 117777.
[33] S. Lü, C. Gao, X. Xu, et al., ACS Appl. Mater. Interfaces 7 (2015) 13029–13037.
[34] Q. Hu, H. Li, E. Archibong, et al., Nat. Biomed. Eng. 5 (2021) 1038–1047.
[35] G. Andrieu, A.H. Tran, K.J. Strissel, G.V. Denis, Cancer Res. 76 (2016) 6555–6567.
[36] F. Sun, Q. Zhu, T. Li, et al., Adv. Sci. 8 (2021) 2002746.
[37] J. Shi, C.R. Vakoc, Mol. Cell 54 (2014) 728–736.
[38] J. Dong, C. Zhu, F. Zhang, Z. Zhou, M. Sun, J. Control. Release 341 (2022) 892–903.